The atomistic level structure for the activated human κ-opioid receptor bound to the full Gi protein and the MP1104 agonist

Amirhossein Mafi[a], Soo-Kyung Kim[a], and William A. Goddard III[a,1]

[a]Materials and Process Simulation Center, California Institute of Technology, Pasadena, CA 91125

Contributed by William A. Goddard III, January 22, 2020 (sent for review June 11, 2019; reviewed by Krzysztof Palczewski and Nagarajan Vaidehi)

The kappa opioid receptor (κOR) is an important target for pain therapeutics to reduce depression and other harmful side effects of existing medications. The analgesic activity is mediated by κOR signaling through the adenylyl cyclase-inhibitory family of Gi protein. Here, we report the three-dimensional (3D) structure for the active state of human κOR complexed with both heterotrimeric Gi protein and MP1104 agonist. This structure resulted from long molecular dynamics (MD) and metadynamics (metaMD) simulations starting from the 3.1-Å X-ray structure of κOR–MP1104 after replacing the nanobody with the activated Gi protein and from the 3.5-Å cryo-EM structure of μOR–Gi complex after replacing the 168 missing residues. Using MD and metaMD we discovered interactions to the Gi protein with strong anchors to two intracellular loops and transmembrane helix 6 of the κOR. These anchors strengthen the binding, contributing to a contraction in the binding pocket but an expansion in the cytoplasmic region of κOR to accommodate G protein. These remarkable changes in κOR structure reveal that the anchors are essential for activation.

G protein activation | metadynamics | biased ligands | pain analgesics | GEnSeMBLE method

Treatment of chronic neuropathic pain is a major challenge in clinical practice (1), because many patients do not experience sufficient pain relief with medications while others experience serious side effects (2). Opioid analgesics such as morphine are strong painkillers, activating opioid receptors in the central nervous system to inhibit pain signals. However, they are not recommended as first-line medications because they evoke such side effects as sedation, physical dependence, addiction, tolerance, and respiratory depression (2). While G protein-mediated signaling is thought to confer analgesia, the potentially lethal side effects of opioids such as fatal respiratory depression are thought to be mainly mediated by μ-opioid receptor (μOR) signaling through the β-arrestin pathway (2). To avoid the side effects associated with arrestin signaling, tremendous efforts are being made to design biased analgesics that favor only G protein-mediated signaling (3). Alternatively, the κ-opioid receptor (κOR) is an important target for developing new pain and depression therapeutics that attenuate the side effects associated with μOR agonists, particularly respiratory depression (4, 5). In particular, μOR and κOR stimulate signaling via the adenylyl cyclase-inhibitory family of G proteins (Gi/o), leading to the analgesic activity (6). Therefore, the detailed interplay between κOR, Gi protein, and a ligand that results in Gi protein activation is crucial for the design of new analgesics. In fact, a major challenge is distinguishing whether a designed ligand serves as an agonist or antagonist. To overcome this challenge, structure-based ligand design can be used to optimize interactions between κOR–Gi–ligand in the active state. Unfortunately, no active state κOR–Gi complex has yet been obtained, hindering the deep understanding of signaling needed to develop new ligands.

We report here this structure: the optimized active state structure for human κOR complexed with full heterotrimeric Gi protein and the high-affinity MP1104 agonist. This three-dimensional (3D) structure should be useful for in silico design of agonists with higher activity and it provides the basis for a deeper understanding of G protein activation.

To predict the structure for this complex we started with the recent 3.1-Å resolution crystal structure of the κOR active state bound to a high-affinity agonist MP1104. This structure was stabilized in the active state with a nanobody (Nb39) (7). Moreover, the resolution of 3.1 Å did not allow identification of 31 amino acid side chains that likely are important (see *Methods*) in recruiting Gi protein. In addition, to obtain the crystal structure of κOR, several modifications were made to facilitate crystallization (7). The most striking modification is the replacement of the intracellular loop 3 (ICL3) with a T4 lysozyme (T4L) protein that stabilized the basal activity of G protein-coupled receptors (GPCRs). It has been shown that altering or mutating residues in the ICL3 of GPCR seems to modify their G protein selectivity, leading to dramatically decreasing transducing activation (8). For instance, mutation of the wild-type sequence from "^{234}AQQQESATTQKAEKEV^{250}" to "^{234}ATSLHGYSVTGPTGSNL^{250}" reduces the transducing activation by 91% in the bovine rhodopsin (8). However, the stimulation of adenylyl cyclase increased by 40% (9) in a chimeric human A_{2a} adrenergic receptor where the wild-type sequence of "^{174}K-L^{396}" including all residues on the ICL3, "^{234}R-W^{362}," were replaced with the wild-type sequence "^{214}I-V^{295}" of human β2 adenosine receptor. Therefore, we speculate that ICL3 of κOR

Significance

We report here the high-resolution structure for the κ-opioid receptor (κOR) with the full Gi protein coupled to it along with a strong agonist, MP1104 bound to form the activated structure. We discovered the Gi protein makes three anchors to the κOR, which most likely results in higher drug efficacy. Our procedure provides the basis for structure-based design of new drugs to mediate pain more effectively while reducing side effects such as physical dependence, tolerance, and respiratory depression. Moreover, it also offers an efficient way to predict the final activated state of G protein–GPCR–agonist complex where the X-ray structures of GPCRs stabilized by a nanobody exist.

Author contributions: A.M. and W.A.G. designed research; A.M. performed research; A.M., S.-K.K., and W.A.G. analyzed data; and A.M., S.-K.K., and W.A.G. wrote the paper.

Reviewers: K.P., University of California, Irvine; and N.V., City Of Hope National Medical Center.

The authors declare no competing interest.

Data deposition: Our optimized structure has been deposited in GitHub, https://github.com/amafi-gpcr/Kappa-Opioid-Receptor-Gi-Protein-MP1104-agonist-Complex-PNAS-2020.

See online for related content such as Commentaries.

[1]To whom correspondence may be addressed. Email: wag@caltech.edu.

This article contains supporting information online at https://www.pnas.org/lookup/suppl/doi:10.1073/pnas.1910006117/-/DCSupplemental.

First published March 3, 2020.

similarly serves a significant role in signaling. Notably, activated GPCRs stabilized by Nbs also differ from those stabilized by their cognate heterotrimeric G protein. Previous observations indicate that GPCRs stabilized by their cognate G proteins undergo a further expansion in their cytoplasmic region in order to open up the space large enough to accommodate G protein α5 helix (10–13). Therefore, regardless of having the active state complex of κOR–MP1104–Nb39, we still need the structure of κOR attached to its cognate G protein to understand the G protein activation mediated by binding of the agonist to κOR.

To obtain the 3D structure for human κOR, we used the active state human κOR–MP1104–Nb39 complex (7) (Protein Data Bank [PDB] ID: 6B73) as the template. However, we removed the Nb39, oleic acid, and the cholesterol resolved in the crystal complex. Then, we replaced the engineered κOR N terminus amino acids with the native residues. This was followed by optimizing the side chains of κOR using the SCREAM method (side-chain rotamer excitation analysis method), which provides an efficient way to orient the residues on different chains for maximal hydrogen bonding (14). The three close subtypes of opioid receptors, including μOR, κOR, and δOR, have 70% identity in the structure of their transmembrane (TM) domains (15). Thus, we used the recent 3.5-Å resolution cryo-EM structure of mouse μOR–DAMGO–nucleotide-free Gi (13) as a template to insert the Gi protein in the κOR–MP1104 complex. To do this, the human κOR–MP1104 was superimposed onto the cryo-EM mouse μOR. However, the mouse μOR–Gi cryo-EM structure did not resolve important amino acid residues 56 to 181 or residues 234 to 240 of the Gαi-alpha helical (AH) domain nor did it resolve the full side chains for several amino acid residues (see *Methods*), including Gαi-E28, E308, E318, and Gβi-D312 that we find to play an important role in coupling the Gi protein to the κOR. Therefore, we built in the AH domain from the recent cryo-EM structure of human rhodopsin complexed with the Gi protein (PDB ID: 6CMO) (16). The side chains in the resulting complex were optimized to maximize the number of interactions between κOR and Gi. Finally, we performed several short (16 to ∼120 ns) molecular metadynamics (metaMD) simulations to find the best pair for each unsatisfied charged residue with the idea of strengthening the interactions between κOR and Gi protein. Then, we examined the stability of interactions and structure by performing classical molecular dynamics (MD) simulations with full membrane and solvent.

We find that the presence of Gi protein alters the binding of MP1104, but it does not change the affinity. A slight change in the binding pose of MP1104 takes place with a further contraction in the κOR extracellular and further expansion in the κOR intracellular region. These changes in the structure are consistent with the general activation mechanism proposed for class A GPCRs, where the contraction in the extracellular region of GPCR is associated with expansion in the intracellular region of GPCRs. However, we discovered that the Gi protein forms strong anchors to ICL1, ICL2, and the cytoplasmic end of TM6. We find that the contraction in the binding site is mostly due to the anchor from the Gi protein to the ICL1 of κOR. In addition, these anchors seem to position the Gαi5 helix so that upon activation it can ascend into the κOR to establish extensive interactions with κOR. We also find that interactions from these anchors and Gαi5 helix to the κOR cause a further expansion in the cytoplasmic region. These findings suggest that strong anchors and Gαi5 interactions with GPCR are essentials for activation and signaling.

Results

Comparison of the Active State κOR–Gi with κOR–Nb39. A full overview of the human κOR–Gi protein–MP1104 complex immersed in the lipid bilayer is shown in *SI Appendix*, Fig. S1. Fig. 1 compares the final structure for the human κOR–MP1104 agonist–nucleotide-free Gi (17) with the active state of the engineered κOR bound to MP1104 agonist stabilized by Nb39. The overall root mean square displacement (RMSD) of $TM^{C\alpha}$ helices between κOR–Gi and κOR–Nb39 is about 1.7 Å (*SI Appendix*, Table S1) where the presence of Gi protein leads to 5.3-Å movement, measuring the distance between $Y119^{2.64}$-$C\alpha^{\kappa OR\text{-}Gi\ protein}$ (the superscript is Ballesteros–Weinstein numbering for GPCRs) (18), taken from ref. 19) and $Y119^{2.64}$-$C\alpha^{\kappa OR\text{-}Nb39}$, of the extracellular (EC) portion of TM2 toward the receptor core (Fig. 1*A*). This movement reduces the volume of binding site from 904.2 $Å^3$ (crystal structure) to 859.4 $Å^3$. We attribute this contraction in the binding site mostly to the strong interaction from Gβi subunit to ICL1 of κOR. To find that such movement of TM2 is statistically significant, we repeated our 200 ns of MD simulations with the Amber14 force field three times using different velocities. We find that in all of our calculations, TM2 tends to move toward the receptor core (*SI Appendix*, Fig. S2 *A–C*). To eliminate the possibility that this contraction in the binding site resulted only from the MD simulation, we also carried out a 200-ns MD simulation on the crystal structure of κOR–Nb39 (Fig. 2*A*). However, since T4L was not resolved and not provided in the crystal structure, we had to replace it with the native ICL3 over the course of the MD simulation. We find that the overall RMSD of $TM^{C\alpha}$ domains between our optimized κOR–Nb39 structure and the crystal structure of κOR–Nb39 is about 1.3 Å. Nonetheless, comparing the optimized structures of κOR–Gi and κOR–Nb39 reveals that Gi protein causes a further 3.6-Å movement of TM2 toward the receptor core (Fig. 2*B*), which consequently contracts the binding site. Finally, to eliminate the probable effects of our chosen force field, we performed a 150-ns MD simulation on the κOR–Gi–MP1104 complex using Charmm36m, which resulted in RMSD = 2.0 Å compared to the crystal κOR–Nb39 complex. Interestingly, a different force field, here Charmm36m, also confirms that Gi protein imposes a 7.4-Å movement of TM2 toward the core, which consequently induces additional contraction in the extracellular domain of κOR (Fig. 2*C*). Thus, despite the force field type, our simulations show that the direct interaction from the Gβi subunit to the ICL1 of κOR causes a pronounced contraction in the binding site.

In addition, we find that interaction between the Gi protein and κOR forces the cytoplasmic segment of TM6 to make a 3.2-Å lateral displacement toward TM7. This leads to opening up the space between TM3 and TM6 (Fig. 1*B*) from 13.7 to 16.9 Å (measuring the distance between K265-Cα and V160-Cα), suggesting that this further 3.2-Å lateral displacement is essential to accommodate the Gαi5 helix. To find that the expansion in the cytoplasmic region of κOR in the presence of Gi protein is statistically significant, we repeated our 200-ns MD simulations with the Amber14 force field three times using different velocities. We find that in all of our calculations, TM6 tends to move away from the TM3 which eventually opens up the space in the receptor core that facilitates Gi protein recruitment (*SI Appendix*, Fig. S2 *D–F*). To ensure that this remarkable change in the cytoplasmic region of κOR is not an artifact of the Amber14 force field, we independently carried out a 150-ns MD simulation on the κOR–Gi complex using Charmm36m (*SI Appendix*, Fig. S3). Strikingly, our calculation confirms that Gi protein indeed imposes a pronounced change in the κOR structure that ends up with opening up the space between TM3 and TM6 from 13.7 to 16.3 Å (Fig. 2*D*) to accommodate Gαi5 helix. This behavior is consistent with previous observations (10–13) that reveal the cytoplasmic end of TM6 in β2 adenosine receptor and μOR structures activated by G protein has a further outward displacement compared to the ones stabilized by Nb (10, 11). Notably, the latter has a similar 3-Å lateral movement toward TM7, which is consistent with our findings for κOR. Overall, these dramatic changes in the κOR structure are consistent with the general activation mechanism proposed for class A GPCRs (20–23) where contraction in the extracellular region of the GPCR is associated with further expansion in the intracellular region of GPCRs.

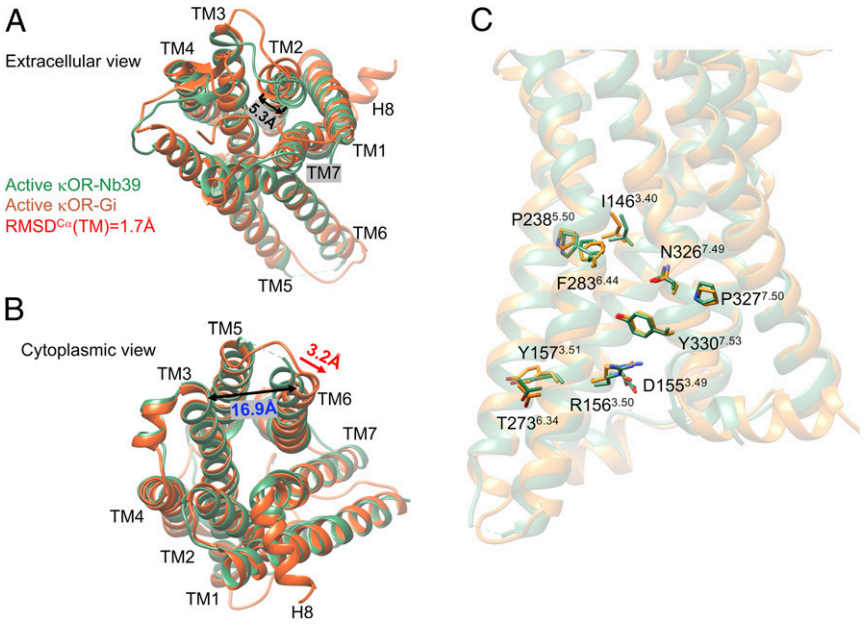

Fig. 1. Structural differences between our κOR stabilized by nucleotide-free Gi protein (orange) using the Amber14 force field and the crystal structure of κOR stabilized by Nb39 (green). (*A*) Extracellular view. (*B*) Cytoplasmic view. (*C*) The conformation of residues in the DRY and NPxxY motifs and other key residues of the κOR in complex with Gi protein (orange) and Nb39 (green). The Gi protein and MP1104 from the κOR–Gi protein complex, and Nb39, and MP1104 as well T4L from the crystal structure (PDB ID: 6B73) are omitted for the sake of clarity.

An important criterion is to compare the conformations of such highly conserved residues as $N^{7.49}P^{7.50}XXY^{7.53}$ as well as $I^{3.40}$, $D^{3.49}$, $R^{3.50}$, $Y^{3.51}$, $P^{5.50}$, and $F^{6.44}$ motifs that have been suggested to be important for GPCR activation (24). Our active state structure of the κOR–Gi protein–agonist complex leads to nearly identical conformations for these highly conserved amino acids in the active state stabilized by Nb39 (7) (Fig. 1*C*). Of these residues, only the conformation of R156 differs slightly between these two structures, because it establishes a polar interaction with C351 in Gαi5 helix in our structure.

Structure of κOR–Gi Complex. A strong polar interaction couples ICL2 of κOR to the αN-β1 loop of Gi protein. The overview of the human κOR–Gi protein–MP1104 complex is described in Fig. 3 along with some important interactions shown in *SI Appendix*, Fig. S4. We find that D168 on ICL2 forms a strong and stable salt bridge with R32 on the GαN-β1 loop of Gαi (Fig. 3*B* and *SI Appendix*, Fig. S4*B*). This ionic coupling is an anchor that coordinates ICL2 to create a network of extensive salt bridges and hydrogen bonds with the Gαi5 helix (Fig. 3*C*). It is well known that the extensive interactions from the Gαi5 helix to the receptor play a pivotal role in G protein binding (25–28). We performed three independent 200-ns MD simulations with Amber14 to examine whether the emergence of this salt bridge is statistically important. Interestingly, we find that all of our simulations feature the strong and stable anchors from R32 on the GαN-β1 loop of Gαi to D168 on ICL2 (*SI Appendix*, Fig. S2 *G–I*). To eliminate the probable effects of the force field, we also carried out a separate 150-ns MD simulation using the Charmm36m force field (*SI Appendix*, Fig. S3) to find that $D168^{ICL2}$ engages in an ionic interaction with the $R32^{GαN\text{-}β1\ loop}$ (*SI Appendix*, Fig. S3*C*). The D168 residue in ICL2 is conserved in μOR, κOR, and δOR (*SI Appendix*, Table S2) (19). To examine whether the μOR–Gi complex also features the same strong couplings, and most importantly to test whether our proposed procedure is able to predict high-resolution complexes of G protein–GPCR–agonist for those GPCRs that were already crystalized and stabilized by a nanobody, we built a new active state structure of mouse μOR–BU72–Gi protein by replacing the Nb39 of the crystal structure (PDB ID: 5C1M) (12) with the Gi protein. Then we optimized this structure in a similar fashion as we described for the κOR–MP1104–Gi complex (*SI Appendix*, Figs. S5 and S6). Strikingly, we find that our model of μOR–BU72–Gi features strong anchoring between the analogous Asp residue in μOR and R32 in the GαN-β1 loop of Gαi (*SI Appendix*, Fig. S6*B*), which induces the Gαi5 helix to engage in extensive interactions with the mouse μOR. To ensure that Gi protein binds to the mouse μOR by forming strong salt bridges to the ICL2, we also optimized the cryo-EM μOR–DAMGO–Gi structure (*SI Appendix*, Fig. S7). Our optimized cryo-EM structure of μOR–DAMGO–Gi confirms that μOR recruits Gi protein by forming strong anchors from the ICL2. These findings show that the anchor between ICL2 and Gi protein is essential for stabilizing the active state complex of opioid receptors.

Our MD simulations find that Gβi also makes a direct ionic contact to the ICL1 of κOR (Fig. 3*D*). A charge–charge interaction is formed between $D312^{Gβi}$ and $K89^{ICL1}$ (*SI Appendix*, Fig. S4*H*) that remains stable during the course of our MD simulation. Forming this salt bridge coordinates $D312^{Gβi}$ to involve another polar interaction with the $K91^{ICL1}$ that frequently becomes a water-mediated interaction (*SI Appendix*, Fig. S4*I*). The same direct interaction between Gβi and κOR is also seen in all of our simulations with Amber14 (Fig. 3*D* and *SI Appendix*, Fig. S2 *G–I*). To examine whether the direct contact between Gβi and ICL1 of κOR is really independent from the force field, we performed another 150-ns MD simulation using Charmm36m. Indeed, we find that $K91^{ICL1}$ establishes a strong and stable charge–charge interaction with $D312^{Gβi}$ (*SI Appendix*, Fig. S3*B*), confirming that the Gβi subunit binds to the ICL1. Although these two Lys residues are conserved in all close subtypes of opioid receptors (*SI Appendix*, Table S2), such interactions were not identified in the cryo-EM μOR–Gi structure (13) since neither the analogous Lys residues nor the $D312^{Gβi}$ were fully resolved within the 3.5-Å resolution. However, optimizing the μOR–Gi complex (*SI Appendix*, Fig. S7), result to emergence of a salt bridge between $K98^{ICL1}$ and $D312^{Gβi}$ (*SI Appendix*, Fig. S7*A*) in the mouse μOR–Gi complex. Interestingly, our active state of μOR–BU72–Gi also

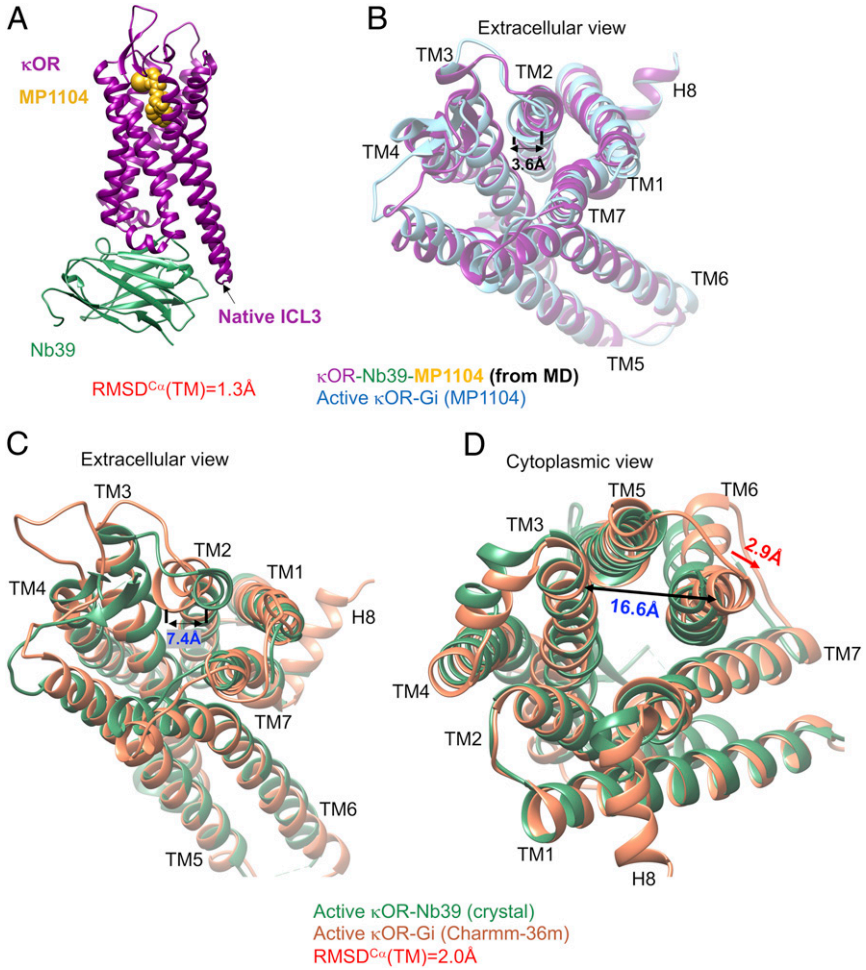

Fig. 2. MD simulations indicate that the Gi protein induces a remarkable contraction in the binding site and further expansion in the cytoplasmic region of the κOR structure. (*A*) The optimized κOR (purple)–MP1104 (yellow)–Nb39 (green) complex using the Amber14 force field. This system contains ∼141 K atoms including: proteins, ligand, 277 POPC, and ∼32,000 water molecules as well as 98 Na^+ and 99 Cl^-. (*B*) Structural comparisons, particularly the binding site, between two optimized κOR structures stabilized by Gi protein (blue) and Nb39 (purple) using the Amber14 force field. Structural comparisons between the optimized κOR stabilized by Gi protein (orange) using the Charmm36m force field and the crystal structure of κOR in complex with Nb39 (green): (*C*) extracellular view and (*D*) cytoplasmic view. The Gi protein, Nb39, and MP1104 as well T4L protein are removed from panels *B*–*D* for the sake of clarity.

reveals that the Gβi subunit forms a strong anchor with $K98^{ICL1}$ (*SI Appendix*, Fig. S6*C*). Thus, direct interactions from Gβi to the conserved Lys residues on ICL1, a second set of anchors, likely play important roles for signaling of opioid receptors.

Interestingly, the cryo-EM structures of the activated GLP1 receptor complexed with the Gs protein (29, 30) shows that D312 in Gβi engages in polar interactions with H171 in the ICL1 of GLP1. Most likely H171 interacts with D312 with its protonated state to form a salt bridge. In addition, the cryo-EM structure of A_{2a} adenosine receptor (A_{2a}AR) (31) complexed with Gs protein also indicates potential polar interactions from residues S35, N36, and Q38 of A_{2a}AR to residues R52, D312, D333, and F335 in Gβ. These observations support our finding that D312 plays a crucial role in coupling the Gβ to ICL1.

We find that electrostatic attractive forces are the main driving force that couples the cytoplasmic end of TM6 to the Gαi RAS-like region. The key interaction that regulates this coupling, is an ionic contact between the protonated N atom of $K265^{6.26}$ at the bottom of TM6 with the negatively charged carboxylate of E318 in Gαi–β6 region (Fig. 3*E* and *SI Appendix*, Fig. S4*J*). This strong electrostatic interaction which is also seen in our other three independent simulations (*SI Appendix*, Fig. S2 *G*–*I*), induces residues in close proximity to form several polar interactions. For instance, the coordinated $K256^{6.26}$ tends to establish a polar interaction with $E308^{Gαi4}$, which occasionally becomes a charge–charge interaction (Fig. 3*E* and *SI Appendix*, Fig. S4*K*). This attraction also induces $E308^{Gαi4}$ to form a hydrogen bond with $S262^{6.23}$. On the other hand, $E308^{Gαi4}$ makes an ionic contact with the protonated N atom of $K314^{Gαi4\text{-}β6\ loop}$ (Fig. 3*E* and *SI Appendix*, Fig. S4 *M* and *O*). Remarkably, these extensive polar interactions regulate both ICL3 and TM6 to involve intense interactions with the Gαi5 helix (Fig. 3*F*). Thus, we find strong polar interactions from Gi protein to ICL3/TM6 of κOR, that constitute the third set of anchors, stabilize the active state complex. To test that this conclusion is independent of the force field, we performed another 150-ns MD simulation with Charmm36m (*SI Appendix*, Fig. S3). We find that a similar network of polar interactions is created between Gαi RAS-like region and ICL3/TM6 of κOR (*SI Appendix*, Fig. S3*D*), where the salt bridge from $K265^{6.26}$ to E318 is the key interaction in this network. Notably, the $K^{6.26}$ is conserved in all close subtypes of opioid receptors (*SI Appendix*, Table S2). Although we find E308 and particularly E318 establish strong interactions with TM6, neither residue was resolved past $C_β$ in the recent cryo-EM μOR–Gi complex (13). Nevertheless, the closest distance between the E318-$C_β$ and the protonated N atom of μOR–$K271^{6.26}$ was 4.8 Å, suggesting these residues would likely take part in an ionic contact.

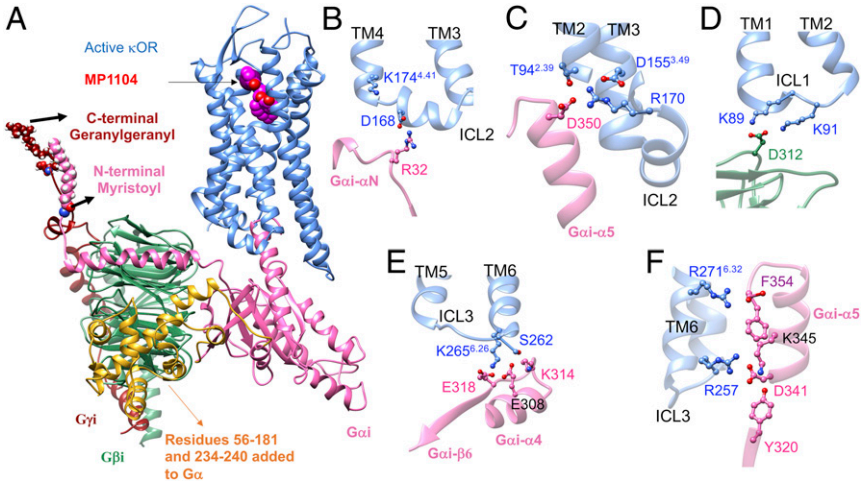

Fig. 3. Structure of the human κOR–GiP–MP1104 complex derived from our MD simulations using the Amber14 force field. (*A*) A side view of the κOR–GiP–MP1104 complex. Cartoon views colored by subunit (blue, κOR; pink, Gαi; green, Gβi; red, Gγi); MP1104 is shown with van der Walls balls. Yellow indicates the missing amino acid residues 56 to 181 and 234 to 240 in the Gα subunit in the cryo-EM (PDB ID: 6DDF) that we added in the simulation. This system contains ~151 K atoms including: proteins, ligand, 277 POPC, and ~32,000 water molecules as well as 98 Na^+ and 100 Cl^-. (*B*) Interaction between Gαi and ICL2 of κOR. (*C*) Interaction of Gαi5 helix with TM2, TM3, and ICL2 of κOR. (*D*) Interaction between Gβi and ICL1 of κOR. (*E*) Interaction of Gαi with the bottom of κOR TM6 and ICL3. (*F*) Interaction of Gαi5 helix with ICL3 and TM6 of κOR.

Indeed, optimization of the complex (*SI Appendix*, Fig. S7*D*) reveals that the activated state of mouse μOR–Gi complex also features a similar strong salt bridge interaction between $K271^{6.26}$ and E318. However, we also find that another anchor emerges between $R263^{ICL3}$ and E318 which is a common feature with our optimized μOR–BU72–Gi structure (*SI Appendix*, Fig. S6*D*).

Our MD simulations indicate that the activated Gαi5 helix involves extensive interactions with the conserved residues in the cytoplasmic domain of human κOR, thereby stabilizing the activated conformation (Fig. 3*C*). It is well known that the Gαi5 helix plays a pivotal role in coupling of G protein to receptors (25–28). We find that Gαi5 binds extensively to the TM2, TM3, and ICL2 by forming a strong network of hydrogen bonds and salt bridges. Here, $R170^{ICL2}$ plays a crucial role in maintaining and regulating this network. $R170^{ICL2}$ engages in a charge–charge interaction with the highly conserved $D155^{3.49}$ (*SI Appendix*, Fig. S4*C*). This salt bridge coordinates the conformation of $R170^{ICL2}$ such that $R170^{ICL2}$ attracts the negatively charged carboxylate group of $D350^{Gαi5}$ (D-5, where "-5" indicates the fifth residue counting from the C terminus of the Gα subunit) to make a persistent salt bridge (*SI Appendix*, Fig. S4*G*). This also induces D-5 to establish a polar interaction with the hydroxyl group of $T94^{2.39}$ (*SI Appendix*, Fig. S4*F*). $T94^{2.39}$ also makes polar contacts with the side chain of $R170^{ICL2}$ (*SI Appendix*, Fig. S4 *D* and *E*). This arginine is a conserved residue in all close subtypes of opioid receptors (*SI Appendix*, Table S2). The cryo-EM structure of μOR–Gi protein also shows that the analogous $R179^{ICL2}$ makes a polar contact with the $D^{3.49}$ and most likely establishes a salt bridge with D-5 (13). The behavior of $R179^{ICL2}$ in the μOR–Gi complex is consistent with the role that its analog plays in the κOR–Gi structure. Indeed, we find that $R179^{ICL2}$ engages in a salt bridge with D-5 in our optimized μOR–BU72–Gi complex (*SI Appendix*, Fig. S6*E*).

Eventually, the Gαi5 terminal carboxylate (F-1) is coupled to the positively charged side chain of $R271^{6.32}$ (Fig. 3*F* and *SI Appendix*, Fig. S4*P*). The $R271^{6.32}$ side chain was not resolved in the crystal structure (7). Although this salt bridge is reasonably stable during the MD simulation, it sometimes becomes a water-mediated interaction. Therefore, to assess the strength of this affinity, we used metaMD simulation (*SI Appendix*, Fig. S8*L*) to find that emergence of the salt bridge stabilizes the complex by reducing the energy by ~1.5 kcal/mol. This moderate level of binding shows why this charge–charge interaction occasionally switches to a water-mediated interaction. Remarkably, the Gαi5 terminal carboxylate in our optimized μOR–BU72–Gi complex involves polar interactions with $R277^{6.32}$ and $N274^{6.29}$. Aside from this, D341 (D-10) on the Gαi5 also couples to R257 on the ICL3, which consequently coordinates K345 (K-6) to form a hydrogen bond with Y320 on the RAS-like region.

MP1104 Agonist Binding. The presence of Gi protein alters the binding of MP1104 but it does not change the total nonbonded interaction energies compared to the complex stabilized by Nb39 (*SI Appendix*, Fig. S9 *A* and *B* and Table S3). We find that the MP1104 agonist binds to the κOR orthosteric pocket, where strong polar interactions lock MP1104 into the human κOR (Fig. 4 *A* and *B* and *SI Appendix*, Figs. S10 and S11 and Table S3). *SI Appendix*, Fig. S10 shows the pharmacophore of the binding sites. The MP1104 agonist primarily engages in a strong and persistent salt bridge from its positively charged amine moiety to the carboxylate group of $D138^{3.32}$ (Fig. 4 *A* and *B* and *SI Appendix*, Figs. S10 *A* and *B* and S11*F* and Table S3). $D^{3.32}$ is conserved in all close subtypes of opioid receptors (*SI Appendix*, Table S2), playing a crucial role in stabilizing the orientation of agonists and antagonists (7, 12, 13, 32–35). In particular, $D^{3.32}$ is an anchoring point for antagonist and agonist association to the κOR binding pocket (36). Here, this salt bridge coordinates the carboxylate group of $D138^{3.32}$ to form a hydrogen bond with $Y320^{7.43}$ (Fig. 4 and *SI Appendix*, Figs. S10 and S11*E*). This hydrogen bond was also identified in the active state κOR–Nb39 complex (7) (*SI Appendix*, Table S3). Indeed, the corresponding link was also observed for the mouse μOR bound to BU72 (12). $Tyr^{7.43}$ plays a crucial role in mediating the binding pocket of the μOR, since it participates in the TM3–TM7 microswitch. Mutating $Y328^{7.43}$ to a Phe dramatically reduces morphine binding affinity (37). We find that MP1104 is further stabilized by forming two hydrogen bonds from furan and carbonyl oxygen atoms to the $Y139^{3.33}$ hydroxyl group (Fig. 4 *A* and *B* and *SI Appendix*, Figs. S10 and S11 *G* and *H*). Another important polar interaction emerges from the $Y312^{7.35}$ hydroxyl group to the MP1104 aromatic ring (*SI Appendix*, Fig. S11 *K* and *L*).

Aromatic interactions between MP1104 and κOR reinforce the agonist binding affinity. $H291^{6.52}$ has an essential role in

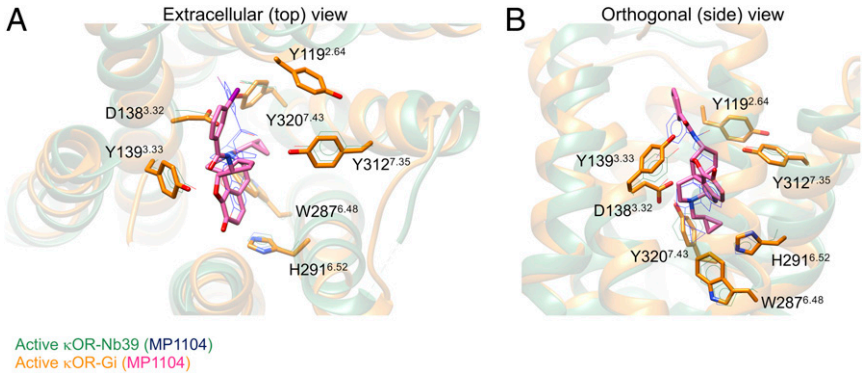

Fig. 4. Comparison of MP1104 agonist binding interactions with the active state κOR in complex with the Gi protein (golden) and Nb39 (green). (*A*) Extracellular view. (*B*) Side view. The amino acid residues and MP1104 in the crystal structure of κOR–Nb39 is described by a wire scheme. Our nucleotide-free Gi protein, water, and ions from the κOR–Gi protein complex, and Nb39 as well T4L fusion proteins from the crystal structure (PDB ID: 6B73) are omitted for the sake of clarity.

creating and regulating the aromatic network interactions. The $H291^{6.52}$ aromatic N atoms make aromatic contacts with the MP1104 ring (Fig. 4*A* and *SI Appendix*, Figs. S11 *A* and *B* and S11 *C* and *D*). $H291^{6.52}$ also induces $W287^{6.48}$ to move toward MP1104. As a result of this movement, $W287^{6.48}$ makes strong aromatic contacts with $H291^{6.52}$ (Fig. 4*B* and *SI Appendix*, Figs. S10 *A* and *B* and S1*B*) and also forms a π–π stacking with the MP1104 aromatic ring (*SI Appendix*, Fig. S11*A*). This network of aromatic interactions stabilizes the conformation of $W287^{6.48}$, ($\chi_1 \sim -70°$ (*gauche*+) and $\chi_2 \sim 110°$ (*gauche*−)) and $H291^{6.52}$, ($\chi_1 \sim -79°$ (*gauche*+) and $\chi_2 \sim -69°$ (*gauche*+)) (*SI Appendix*, Fig. S12 *A–D*). The same χ_2 value was reported for the activated structure of the mouse μOR bound to BU72 (12). $W287^{6.48}$ has been shown to play a key part in the activation of A_{2a}AR (38) and rhodopsin (39).

Discussion

Our MD simulations reveal that after G protein recruitment to the GPCR, there is a further contraction in the GPCR binding site while there is increased expansion in the cytosolic region of GPCR that facilitates stabilizing the complex by creating the extensive interactions from G protein to the cytoplasmic region of GPCR. These remarkable rearrangements of the κOR by G protein, transform the receptor toward its actual activated state. These GPCR structural changes are consistent with the conserved activation mechanism for many class A GPCRs (20–23), where the expansion of the intracellular part of the GPCR coincides with contraction of the GPCR binding site. Therefore, our finding suggests that Nb39 is able to shift κOR structure from the inactive state up to an intermediate state, where the cytoplasmic region is not fully open, and the binding site is not fully contracted.

Our simulations show that anchors from the G protein to κOR are essential for activation of κOR and for stabilizing the active state complex. Our final active state complex includes two main interactions: 1) strong anchors from the G protein to both ICL1 and ICL2 and to the end of TM6; and 2) extensive interactions from the Gαi5 helix to the cytoplasmic region of κOR.

It is generally thought that Gαi5 helix has a pivotal role in stabilizing the active state GPCR–G protein complex. However, we have shown that anchors along with extensive interactions from Gαi5 evolve the structure to reach the final activated state, indicating the significant and perhaps essential role of anchors for activating κOR. This discovery of the role of anchors provides insight into the activation mechanism. It speculates that the agonist binds first to inactive GPCR to partially open up the cytoplasmic region by opening TM3–TM6 coupling. In this scenario, the Gi protein then approaches the GPCR by forming anchors to ICL1, ICL2, and the end of TM6. At this stage, the role of three anchors would align the Gαi5 helix just right to be inserted into the GPCR. Once Gαi5 helix gets inserted into the GPCR, it further opens up the distance between TM3 and TM6 to establish extensive polar interactions. Further expansion in the cytoplasmic region of GPCR coincides with further contraction of the GPCR binding site.

Given the strength of the three anchors, this suggests that the G protein binds firsts, opening the TM3–6 coupling and partially inserting the Gαi5 helix, followed by agonist binding to complete the activation. This provides an alternative scenario to the generally accepted mechanism in which agonist binds first and recruits the G protein to be activated.

Besides, we also proposed an approach to predict a high-resolution structure of G protein–GPCR–agonist complex, using available GPCR structures that already were crystalized by an active-state stabilizing nanobody. The resulting high-resolution structures definitely facilitate discovery of new drugs acting on GPCRs for different applications.

Methods

Refining the Activated Human κOR in Complex with MP1104 Agonist. A total of 31 residues were not fully resolved in the crystal structure of human κOR bound to MP1104 agonist (PDB ID: 6B73) (7), including L51, I54, R86, S188, S192, K200, V201, R202, D206, V207, D216, D217, M226, L251, K254, R257, S262, R263, E264, K265, R267, L269, R270, R271, E297, T302, S305, I328, L329, M336, and R339. Of these residues, R257, S262, and R271 engage in important polar interactions with Gi protein. We added these missing atoms/side chains using Swiss-Pdbviewer (40), where during the process we also reconstructed the side chains. Then, we replaced the engineered κOR N terminus with the native residues from UNIPROT ID: 41145. We also removed the T4L protein and added the amino acid sequence of ICL3 instead. We reconstructed the disulfide bridge between $C131^{3.25}$ and C210 of EC2 manually by selecting new rotamers for these residues to have perpendicular Cβ-S-S-Cβ dihedral angles. Then, we subjected these conformations to 10 cycles of simulated annealing, in which all of the residues in the loops were heated from 50 to 600 K and cooled back to 50 K over 10 ps of simulation. We repeated this heat-and-quench cycle 10 times. During this process, all other residues in TM domains were fixed. We extracted the final structure of this process for further minimization. Subsequently, we exploited SCREAM (14) and GEnSeMBLE (41) methods to refine the side chain of all residues in order to obtain the minimized structure. We used this minimized structure for building the κOR–Gi protein complex.

Gi Protein Preparation. The following 35 residues were not fully resolved or were missing in the cryo-EM structure (PDB ID: 6DDF): residues L5, E28, E43, I55, E207, N241, K270, E275, K279, K280, I285, C305, E308, E318, T327, D337, and D350 in Gαi; residues K23, C25, S31, R46, E130, R214, M217, N237, C271, N237, C271, K301, D312, and C317 in Gβi; and residues D26, D48, S57, and E58, in Gγi.

Of these residues, E308$^{G\alpha i}$, E318$^{G\alpha i}$, and D312$^{G\beta i}$ involve forming anchors with ICLs of κOR. We added these missing residues using Swiss-Pdbviewer (40), where during the process we also reconstructed the side chains.

The entire amino acid residues in the AH domain of the Gαi subunit (PDB ID: 6DDF) (13), residues 56 to 181 and 234 to 240, were all missing. These missing residues were added by superimposing the cryo-EM structure of Gαi complexed with rhodopsin (PDB ID: 6CMO) (16) to the cryo-EM structure of Gαi complexed with the mouse μOR. We used the Needleman–Wunsch sequence alignment algorithm (42) with the BLOSUM-62 matrix, which is incorporated in the UCSF chimera software package (43). Then, we minimized the structure including the connections between residues in Ras-like and AH domains using the conjugated gradients method with 500 steps. During the energy minimization process, all heavy atoms in the Ras-like domain were restrained with a strong harmonic force constant of ∼24 kcal·mol^{-1}·Å^{-2} to avoid any undesirable changes in the original structure of Gαi.

Eventually, we extended the sequence of residues in the N terminus of the Gαi, and C terminus of the Gγi using Prime (Schrödinger) in order to add the N-terminal myristoyl, as well as C-terminal geranylgeranyl to Gαi and Gγi, respectively.

Modeling of Human κOR–MP1104–Nb39 Complex. To build a complex we used chain A of the crystal structure, but we had to make two modifications: 1) we replaced the T4L protein with the native ICL3 sequence because T4L was not resolved or provided. 2) Since there are missing residues/parts in the Nb39 of chain A, we modeled the missing parts, mostly backbone atoms, using the Nb39 structure provided in chain B. To do this, we superimposed two Nb39 structures and then added the required residues to fill the gaps in the Nb39 of chain A. Subsequently, we fixed these missing atoms/side chains using Swiss-Pdbviewer (40), where during the process we also reconstructed the side chains. Eventually, we replaced our modified human κOR to the one provided in the crystal structure.

Modeling of Human κOR–MP1104–Gi Complex. To build a complex, we superimposed the refined human κOR–MP1104 to the refined cryo-EM structure of mouse μOR–DAMGO–Gi using the Needleman–Wunsch sequence alignment algorithm (42). To locate and optimize the interactions between human κOR and Gi protein, we performed 1 ns (50 cycles) of simulated annealing, in which the system was heated from 25 to 600 K with a sequence of 25, 100, 310, 450, 600 and cooled back to 310 K over 50 ps of simulation. In this calculation, we placed harmonic restraints on all backbone and agonist heavy atoms with a force constant of ∼9.6 kcal·mol^{-1}·Å^{-2}. However, to optimize the conformation of the ICL3, no restraints were placed on the backbone atoms.

System Environment Preparation. We used our preequilibrated palmitoyl-oleoyl-phosphatidylcholine (POPC) bilayer structure (44), which was used to study the interaction between human somatostatin receptor 5 (h-SSTR5) and Gi protein. To exploit this preequilibrated lipid structure, including 277 POPC molecules, we aligned the refined human κOR–MP1104–Gi and human κOR–MP1104–Nb39 to the h-SSTR5. Subsequently, we used GROMACS to place the membrane and protein in a cubic box of 100 × 100 × 150 A^3 in such a way that the extracellular region above the POPC membrane was filled with ∼2 nm thick preequilibrated water slab at 298 K (45). The intracellular region below the membrane bilayer was also filled with preequilibrated water. Then, sodium and chloride ions were added to maintain the electronic neutrality of the system at a salt concentration of 100 mM. The final box contained ∼32,300 water molecules.

All molecules were parameterized using Amber force fields during simulations. The behavior of proteins was described by the Amber14 (46) and parameters for the POPC were borrowed from the LIPID17, which is incorporated in Ambertools 16 (47). The parameters to treat the N-terminal myristoyl and C-terminal geranylgeranyl were borrowed from the studies by van Keulen et al. (48), and Khouri et al. (49), respectively. The carboxymethylation of the lipid linkages as well as the ligand, MP1104, were described by the parameters obtained from the generalized Amber force field (GAFF) (50) using ACPYPE (51) and Antechamber16 (52). The partial charges for these two were assigned with the semiempirical AM1-BCC model (53), which is incorporated in UCSF chimera (43). Water was described by the TIP3P (54) model.

To examine whether our findings are independent from the applied force field, we also carried out a separate equilibration on the human κOR–MP1104–Gi complex using the Charmm36m force field. For this calculation, proteins including their lipid linkage, POPC, ions, were described by the parameters set by Charmm36m (55). Water was described by the TIP3P (54) model. The ligand was parameterized by the ParamChem server (56, 57).

Equilibration. Subsequent to the preequilibration steps that are described in *SI Appendix*, we extracted the trajectory at ∼61 ns that corresponds to the minimum of free energy resulting from step 6 (*SI Appendix*). We included the N-terminal myristoyl to Gαi and C-terminal geranylgeranyl to Gγi. Then, we minimized the systems including κOR–MP1104–Gi, κOR–MP1104–Nb39, and κOR–MP1104–Gi (Charmm36m), by 5,000 steps of energy minimization with the steepest descent algorithm. Subsequently, we prepared these systems for the final equilibration by performing short NVT (constant particles, volume, and temperature) for ∼75 ps, and NPT (constant number of particles, pressure, and temperature) for ∼350 ps, MD simulations, where positional restraints were placed on the heavy atoms with a force constant of 9.6 kcal·mol^{-1}·Å^{-2} and gradually reduced to 0 kcal·mol^{-1}·Å^{-2} during the course of simulations. Eventually, we carried out a 200 ns of NPT simulation on κOR–MP1104–Gi, κOR–MP1104–Nb39 structures and a 150-ns NPT simulation on the κOR–MP1104–Gi (Charmm36m), without applying any restraints on the structures to relax the systems and also examine the stability of interactions. We used the results of these MD simulations for analyzing and producing the figures in this study. We also repeated the same procedures three additional times on the κOR–MP1104–Gi complex using Amber14. Besides, in order to have a fair comparison between the MP1104 binding pose in the presence of Gi and Nb39, we performed another round of energy minimization followed by preparations and final equilibration (30-ns MD simulations) on the κOR–MP1104–Nb39 complex, to make sure the MP1104 binding pose obtained from the crystal structure was not changed significantly due to the modifications that we made.

Conclusion

We report the discovery that G protein makes strong anchors to the three intracellular loops of κOR, which modifies the agonist binding site and orients the Gαi5 helix for insertion upon activation. This binding site may be very useful for designing new selective agonists for κOR and for determining how different the binding sites are for biased versus nonbiased ligands to κOR.

The very specific predictions of the residues involved in forming the anchors should provide numerous targets for mutational studies to validate and refine the predicted anchors between the G protein and κOR.

ACKNOWLEDGMENTS. This work was supported by the Gwangju Institute of Science and Technology (GIST)–Caltech Research Collaboration Project through a grant provided by GIST for 2016–2018. It was also funded by grants from the China Scholarship Council and by gifts to the Materials and Process Simulation Center. The computational resources were provided by a Defense-University Research Instrumentation Project-Office of Naval Research grant to W.A.G.

1. N. Singla *et al.*, A randomized, Phase IIb study investigating oliceridine (TRV130), a novel μ-receptor G-protein pathway selective (μ-GPS) modulator, for the management of moderate to severe acute pain following abdominoplasty. *J. Pain Res.* **10**, 2413–2424 (2017).
2. A. Manglik *et al.*, Structure-based discovery of opioid analgesics with reduced side effects. *Nature* **537**, 185–190 (2016).
3. S. M. DeWire *et al.*, A G protein-biased ligand at the μ-opioid receptor is potently analgesic with reduced gastrointestinal and respiratory dysfunction compared with morphine. *J. Pharmacol. Exp. Ther.* **344**, 708–717 (2013).
4. Z. Z. Pan, μ-Opposing actions of the κ-opioid receptor. *Trends Pharmacol. Sci.* **19**, 94–98 (1998).
5. M. R. Bruchas, B. L. Roth, New technologies for elucidating opioid receptor function. *Trends Pharmacol. Sci.* **37**, 279–289 (2016).
6. R. Al-Hasani, M. R. Bruchas, Molecular mechanisms of opioid receptor-dependent signaling and behavior. *Anesthesiology* **115**, 1363–1381 (2011).
7. T. Che *et al.*, Structure of the nanobody-stabilized active state of the kappa opioid receptor. *Cell* **172**, 55–67.e15 (2018).
8. S. Acharya, Y. Saad, S. S. Karnik, Transducin-α C-terminal peptide binding site consists of C-D and E-F loops of rhodopsin. *J. Biol. Chem.* **272**, 6519–6524 (1997).
9. B. K. Kobilka *et al.*, Chimeric alpha 2-,beta 2-adrenergic receptors: Delineation of domains involved in effector coupling and ligand binding specificity. *Science* **240**, 1310–1316 (1988).
10. S. G. Rasmussen *et al.*, Structure of a nanobody-stabilized active state of the β(2) adrenoceptor. *Nature* **469**, 175–180 (2011).
11. S. G. Rasmussen *et al.*, Crystal structure of the β2 adrenergic receptor-Gs protein complex. *Nature* **477**, 549–555 (2011).
12. W. Huang *et al.*, Structural insights into μ-opioid receptor activation. *Nature* **524**, 315–321 (2015).

13. A. Koehl *et al*., Structure of the μ-opioid receptor-G_i protein complex. *Nature* **558**, 547–552 (2018).
14. V. W. Tak Kam, W. A. Goddard, 3rd, Flat-bottom strategy for improved accuracy in protein side-chain placements. *J. Chem. Theory Comput.* **4**, 2160–2169 (2008).
15. M. Waldhoer, S. E. Bartlett, J. L. Whistler, Opioid receptors. *Annu. Rev. Biochem.* **73**, 953–990 (2004).
16. Y. Kang *et al*., Cryo-EM structure of human rhodopsin bound to an inhibitory G protein. *Nature* **558**, 553–558 (2018).
17. A. Mafi, S. S Kim, W. A. Goddard, Kappa-Opioid-Receptor-Gi-Protein-MP1104-agonist-Complex. GitHub. https://github.com/amafi-gpcr/Kappa-Opioid-Receptor-Gi-Protein-MP1104-agonist-Complex-PNAS-2020. Deposited 17 February 2020.
18. J. A. Ballesteros, H. Weinstein, *Methods in Neurosciences* (Elsevier, 1995), vol. 25, pp. 366–428.
19. G. Pándy-Szekeres *et al*., GPCRdb in 2018: Adding GPCR structure models and ligands. *Nucleic Acids Res.* **46**, D440–D446 (2018).
20. G. Milligan, Insights into ligand pharmacology using receptor-G-protein fusion proteins. *Trends Pharmacol. Sci.* **21**, 24–28 (2000).
21. R. Nehmé *et al*., Mini-G proteins: Novel tools for studying GPCRs in their active conformation. *PLoS One* **12**, e0175642 (2017).
22. T. Warne, P. C. Edwards, A. S. Doré, A. G. W. Leslie, C. G. Tate, Molecular basis for high-affinity agonist binding in GPCRs. *Science* **364**, 775–778 (2019).
23. S. Lee, A. K. Nivedha, C. G. Tate, N. Vaidehi, Dynamic role of the G protein in stabilizing the active state of the adenosine A2A receptor. *Structure* **27**, 703–712.e3 (2019).
24. K. P. Hofmann *et al*., A G protein-coupled receptor at work: The rhodopsin model. *Trends Biochem. Sci.* **34**, 540–552 (2009).
25. R. Onrust *et al*., Receptor and betagamma binding sites in the α subunit of the retinal G protein transducin. *Science* **275**, 381–384 (1997).
26. W. M. Oldham, N. Van Eps, A. M. Preininger, W. L. Hubbell, H. E. Hamm, Mechanism of the receptor-catalyzed activation of heterotrimeric G proteins. *Nat. Struct. Mol. Biol.* **13**, 772–777 (2006).
27. W. M. Oldham, H. E. Hamm, Heterotrimeric G protein activation by G-protein-coupled receptors. *Nat. Rev. Mol. Cell Biol.* **9**, 60–71 (2008).
28. N. P. Skiba, H. Bae, H. E. Hamm, Mapping of effector binding sites of transducin α-subunit using G α t/G α i1 chimeras. *J. Biol. Chem.* **271**, 413–424 (1996).
29. Y.-L. Liang *et al*., Phase-plate cryo-EM structure of a biased agonist-bound human GLP-1 receptor-Gs complex. *Nature* **555**, 121–125 (2018).
30. Y. Zhang *et al*., Cryo-EM structure of the activated GLP-1 receptor in complex with a G protein. *Nature* **546**, 248–253 (2017).
31. J. García-Nafría, Y. Lee, X. Bai, B. Carpenter, C. G. Tate, Cryo-EM structure of the adenosine A_{2A} receptor coupled to an engineered heterotrimeric G protein. *eLife* **7**, e35946 (2018).
32. G. Fenalti *et al*., Molecular control of δ-opioid receptor signalling. *Nature* **506**, 191–196 (2014).
33. S. Granier *et al*., Structure of the δ-opioid receptor bound to naltrindole. *Nature* **485**, 400–404 (2012).
34. A. Manglik *et al*., Crystal structure of the μ-opioid receptor bound to a morphinan antagonist. *Nature* **485**, 321–326 (2012).
35. H. Wu *et al*., Structure of the human κ-opioid receptor in complex with JDTic. *Nature* **485**, 327–332 (2012).
36. G. Subramanian, M. G. Paterlini, D. L. Larson, P. S. Portoghese, D. M. Ferguson, Conformational analysis and automated receptor docking of selective arylacetamide-based κ-opioid agonists. *J. Med. Chem.* **41**, 4777–4789 (1998).
37. K. Raynor *et al*., Pharmacological characterization of the cloned kappa-, delta-, and mu-opioid receptors. *Mol. Pharmacol.* **45**, 330–334 (1994).
38. F. Xu *et al*., Structure of an agonist-bound human A2A adenosine receptor. *Science* **332**, 322–327 (2011).
39. J. Standfuss *et al*., The structural basis of agonist-induced activation in constitutively active rhodopsin. *Nature* **471**, 656–660 (2011).
40. N. Guex, M. C. Peitsch, SWISS-MODEL and the Swiss-Pdb Viewer: An environment for comparative protein modeling. *Electrophoresis* **18**, 2714–2723 (1997).
41. J. K. Bray, R. Abrol, W. A. Goddard, 3rd, B. Trzaskowski, C. E. Scott, SuperBiHelix method for predicting the pleiotropic ensemble of G-protein-coupled receptor conformations. *Proc. Natl. Acad. Sci. U.S.A.* **111**, E72–E78 (2014).
42. S. B. Needleman, C. D. Wunsch, A general method applicable to the search for similarities in the amino acid sequence of two proteins. *J. Mol. Biol.* **48**, 443–453 (1970).
43. E. F. Pettersen *et al*., UCSF Chimera–A visualization system for exploratory research and analysis. *J. Comput. Chem.* **25**, 1605–1612 (2004).
44. S. S. Dong, W. A. Goddard, 3rd, R. Abrol, Conformational and thermodynamic landscape of GPCR activation from theory and computation. *Biophys. J.* **110**, 2618–2629 (2016).
45. M. J. Abraham *et al*., GROMACS: High performance molecular simulations through multi-level parallelism from laptops to supercomputers. *SoftwareX* **1**, 19–25 (2015).
46. C. J. Dickson *et al*., Lipid14: The amber lipid force field. *J. Chem. Theory Comput.* **10**, 865–879 (2014).
47. D. A. Case *et al*., *AMBER16* (University of California, San Francisco, 2018).
48. S. C. van Keulen, U. Rothlisberger, Effect of N-terminal myristoylation on the active conformation of $G\alpha_{i1}$-GTP. *Biochemistry* **56**, 271–280 (2017).
49. G. A. Khoury, J. P. Thompson, J. Smadbeck, C. A. Kieslich, C. A. Floudas, Forcefield_PTM: Ab initio charge and AMBER forcefield parameters for frequently occurring post-translational modifications. *J. Chem. Theory Comput.* **9**, 5653–5674 (2013).
50. J. Wang, R. M. Wolf, J. W. Caldwell, P. A. Kollman, D. A. Case, Development and testing of a general amber force field. *J. Comput. Chem.* **25**, 1157–1174 (2004).
51. A. W. Sousa da Silva, W. F. Vranken, ACPYPE - AnteChamber PYthon Parser interfacE. *BMC Res. Notes* **5**, 367 (2012).
52. J. Wang, W. Wang, P. A. Kollman, D. A. Case, Automatic atom type and bond type perception in molecular mechanical calculations. *J. Mol. Graph. Model.* **25**, 247–260 (2006).
53. A. Jakalian, D. B. Jack, C. I. Bayly, Fast, efficient generation of high-quality atomic charges. AM1-BCC model: II. Parameterization and validation. *J. Comput. Chem.* **23**, 1623–1641 (2002).
54. W. L. Jorgensen, J. Chandrasekhar, J. D. Madura, R. W. Impey, M. L. Klein, Comparison of simple potential functions for simulating liquid water. *J. Chem. Phys.* **79**, 926–935 (1983).
55. J. Huang *et al*., CHARMM36m: An improved force field for folded and intrinsically disordered proteins. *Nat. Methods* **14**, 71–73 (2017).
56. K. Vanommeslaeghe *et al*., CHARMM general force field: A force field for drug-like molecules compatible with the CHARMM all-atom additive biological force fields. *J. Comput. Chem.* **31**, 671–690 (2010).
57. K. Vanommeslaeghe, A. D. MacKerell, Jr, Automation of the CHARMM General Force Field, Automation of the CHARMM general force field (CGenFF) I: Bond perception and atom typing. *J. Chem. Inf. Model.* **52**, 3144–3154 (2012).